World Academy of Science, Engineering and Technology
International Journal of Geotechnical and Geological Engineering
Vol:10, No:10, 2016

Laser Ultrasonic Diagnostics and Acoustic Emission Technique for Examination of Rock Specimens under Uniaxial Compression

Elena B. Cherepetskaya, Vladimir A. Makarov, Dmitry V. Morozov, Ivan E. Sas

***Abstract*—**Laboratory studies of the stress-strain behavior of rocks specimens were conducted by using acoustic emission and laser-ultrasonic diagnostics. The sensitivity of the techniques allowed changes in the internal structure of the specimens under uniaxial compressive load to be examined at micro- and macro scales. It was shown that microcracks appear in geologic materials when the stress level reaches about 50% of breaking strength. Also, the characteristic stress of the main crack formation was registered in the process of single-stage compression of rocks. On the base of laser-ultrasonic echoscopy, 2D visualization of the internal structure of rocky soil specimens was realized, and the microcracks arising during uniaxial compression were registered.

***Keywords*—**Acoustic emission, geomaterial, laser ultrasound, uniaxial compression.

I. Introduction

THE modern underground construction technologies require full information about soil conditions so as to improve the reliability of underground structures [1], [2]. Therefore, the mechanical behavior of rocks under load is very important. However, the evaluation of rock properties is quite a laborious task because of rock anisotropy, heterogeneity, and defects of various sizes [3], [4]. In this regard, model experiments are of particular interest to study the processes of crack formation in materials whose physical and mechanical properties are similar to those of rocks.

Among geologic materials, quartz is one of the most suitable for this purpose, primarily due to its variability and a relatively simple structure. Quartz is an important constituent of the Earth's crust: many rocks contain up to 20% of quartz [5], [6].

This work was aimed at studying changes in the internal structure of quartz crystals under uniaxial compressive load using acoustic emission and laser-ultrasonic nondestructive testing techniques. We also studied acoustic emissions produced in specimens of basalts with different textures under uniaxial load. Like quartz, basalt is abundant in the earth crust; it is widely used as an acid-resistant building and facing material, and as a raw material for stone casting, etc.

E. B. Cherepetskaya is with the National University of Science and Technology, Russia (phone: +7(916)6041012; e-mail: echerepetskaya@mail.ru).

V. A. Makarov is with International Laser Center of M. V. Lomonosov Moscow State University (e-mail: vamakarov@phys.msu.ru).

D. E. Morozov and I. E. Sas are with the National University of Science and Technology, Russia (e-mail: moroz_off_123@mail.ru, ivan_sas@bk.ru).

II. Material and Methods

We investigated specimens of quartz with trigonal crystal structure, 5.01x2.55x2.55 cm in size (the long side of specimens oriented along the crystallographic axis Y). The material had no discontinuities before testing; the surface dislocation density was no more than 40 cm^{-2}.

Specimens of basalt were taken at Mutnovsky Volcano located on the northeastern tip of the South Kamchatka volcanic zone in Russia. The basement of the volcano is made up of Palaeogene to Lower and Middle Pleistocene volcanogenic sedimentary and volcanogenic deposits [9], [10]. The basalts found there have similar chemical composition and petrographic characteristics. They are grey to dark grey porphyries with glassy or fine-grained groundmass with vitrophyric, tholeiitic, and microdoleritic texture. The total amount of phenocrysts varies from 10 to 40 vol.%. Olivine phenocrysts in the form of idiomorphic crystals are present in two generations or serial porphyritic enclaves [11], [12]. The olivine phenocryst content varies from individual grains to 3-5%. Olivine usually contains no inclusions; only rarely olivine rims have outgrowths of small (0.05 mm) plagioclase tablets or roundish glassy groundmass enclaves devoid of fine-grained oxide facies, which are characteristics of the groundmass of the described rocks. Olivine itself may form rounded growths in the central parts of large porphyritic enclaves of plagioclase or microporphyritic segregations confined to the marginal parts of plagioclase phenocrysts. Sometimes olivine inclusions are observed in clinopyroxene, too [13]. Plagioclase is present in porphyritic and glomeroporphyritic segregations and forms two generations or serial porphyritic enclaves. Plagioclase content varies from 5-7 to 25-30 vol.%. Clinopyroxene phenocrysts are fresh short columnar crystals. Their percentage varies in a very wide range: from single grains to 5-7 vol.%, reaching sometimes 15 vol.% [13]. The peripheral margins of clinopyroxene phenocrysts sometimes host microporphyritic inclusions of plagioclase and small crystals of an oxide mineral. Note that the basalts have quite large crystals of this oxide mineral, which is magnetite or titanomagnetite, judging by the form and reflectivity. These crystals look like microporphyritic enclaves seated in the groundmass in which ultrafine grains of this mineral (a few hundredths of millimeter in size) are dissipated.

In our study, basalt specimens were 30x30x58 mm in size and had approximately the same density ρ = 2.60 g/cm^3; the specimens represented different textural varieties of basalt.

The following physical properties of the material were measured before testing: density $\rho = 2.64g/cm^3$; longitudinal wave velocity V_p; transverse wave velocity V_s; and uniaxial compressive strength R_c for some specimens (Table I).

TABLE I
PHYSICAL AND MECHANICAL PROPERTIES OF MATERIAL

Axis	$V_p, m/s$	$V_s, m/s$	σ_c, MPa
X	6182	4089	155
Y	6303	4113	160
Z	6779	4458	185

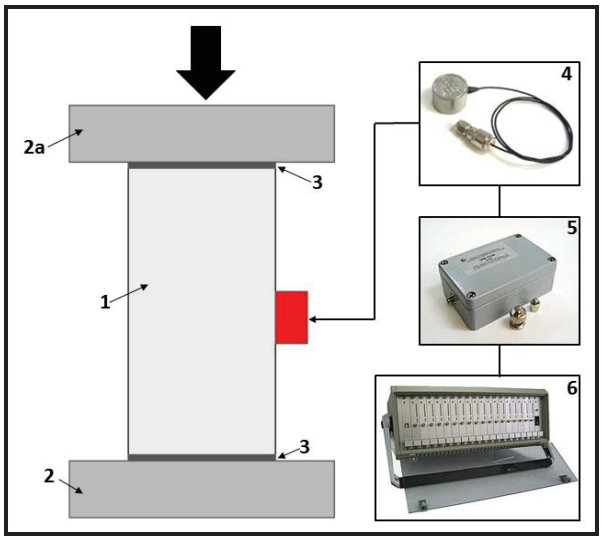

Fig. 1 Scheme of loading of specimens and simultaneous recording of AE: 1) a specimen; 2) the lower fixed plate of press; 2a) the upper movable plate; 3) film to prevent friction; 4) AE sensor; 5) signal amplifier; 6) computing unit

The rest of the specimens were subjected to uniaxial compression. A manual press for compressive strength testing was used (Fig. 1). The rate of loading was 3 kN/s. As a specimen was loaded, acoustic emissions (AE) were recorded by using an *SDS 1008* system (Fig. 1); a broadband piezoelectric ceramic sensor was fixed to specimens. The gain factor of the electroacoustic path was 75 dB.

The occurrence time of AE events (pulses) and the AE counts *N* (*N* is the number of times the acoustic emission signal exceeds a preset threshold) were registered.

The internal structure of the specimens was studied by using GEOSKAN-2MU [7], [8], an automated laser-ultrasonic structuroscope, operating in pulse echo mode. The structuroscope can detect such defects as pores, microcracks, and foreign inclusions. The technique is based on the registration of acoustic pulses reflected from inhomogeneities in a medium. The thickness of a specimen can be determined from Δt_h, which is the time difference between the arrival of the signals reflected from the lower side of the specimen and the reference arrival:

$$h = c_l \Delta t_h / 2, \quad (1)$$

where c_l is the velocity of elastic longitudinal waves.

Similarly, the distance between the defect and the surface can be found:

$$h_d = c_l \Delta t_d / 2 \quad (2)$$

Δt_d is the delay between the signal reflected from a defect and the reference signal. The inaccuracy of calculations, which is determined by the inaccuracy of measurements of *h* and corresponding time intervals, is less than 0.5%.

The short duration of sounding signals allows defects to be detected at a depth of more than 0.2 mm. The "dead" zone is minimal at that. If scanning over the top surface of a specimen with a step of less than 2 mm, it is possible to obtain a 2D image of the internal structure of the specimen.

III. RESULTS

During the gradual application of load, the maximum stress was 78.4 MPa, which is 52% of breaking load. The dependence of the ratio of the AE count (*N*) to the maximum AE count (N_{max}) on the applied stress σ (Fig. 2) shows that the AE count *N* increases and local structural defects are formed in the specimen at the early stages of gradual mechanical loading, when the applied stress is some 10-35% of breaking load. Large defects occur at a stress of 50 MPa and more, when small local defects coalesce into main cracks. When kept under constant load at the end of the experiment, the specimens show an abrupt increase in AE activity, which also is testimony that defects are caused by mechanical loading. In this case, AE activity is due to the presence of defects in the specimen, not the increasing mechanical load.

Laser ultrasonic examination was conducted to confirm the above findings; numerous defects resulting from mechanical loading were identified and localized. The visualization of the internal structure of the specimens allowed the defects to be divided into the following groups:

- local defects no more than 2.5 mm long in plane;
- local defects no more than 6 mm long in plane;
- large defects over 10 mm long in plane.

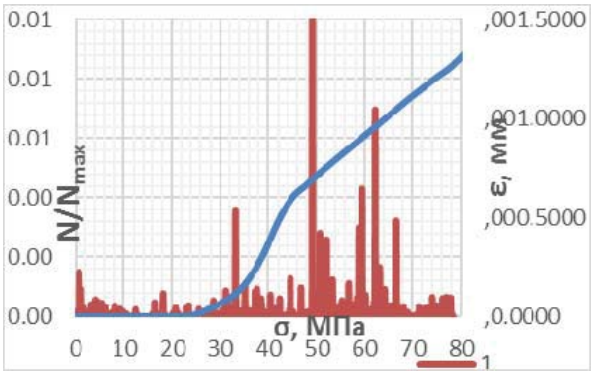

Fig. 2 Dependence of N-to-N_{max} ratio on the stress, based the results of mechanical loading experiment

It should be noted that not only defects on the specimen surfaces, which were in contact with the press plates, were detected, but also main cracks. Thus, the mechanical loading caused not only the deformation of the material and the formation of local defects, but also changes in its overall properties and behavior.

The results of the study of acoustic emissions in basalts of three textural types are shown in Fig. 4. The first type of the curves (Fig. 4 (a)) is chiefly characteristic of high-magnesia basalts with a large amount of olivine phenocrysts (25-40%) evenly distributed in the groundmass composed of plagioclase (40%) and pyroxene (60%). Olivine crystals are large (from 0.5 to 6 mm) and fractured; crystals of plagioclase and pyroxene are 0.1 mm and 0.02 mm in size, respectively. During the gradual application of load, the AE count uniformly increases; AE amplitudes increase tenfold by the end of the test. This is most probably due to the large amount of fractured olivine. The bandwidth distribution of the ratio of the maximum AE signal count to the rate of loading is as follows: the number of the low-frequency signals is half the number of the mid-frequency signals, which in turn is approximately equal to the number of high-frequency signals. These relations remain unchanged if the rocks have the same porosity and their typical sizes vary insignificantly. As this parameter increases twofold, the number of high-frequency signals decreases twofold. This phenomenon can be explained as follows: the compression of pores occurs at the initial stages of gradual mechanical loading, and the spatial parameters correspond to the wavelengths of the mid- and high-frequency ranges. Then, microcracks begin to form and the energy is emitted in the low-frequency range.

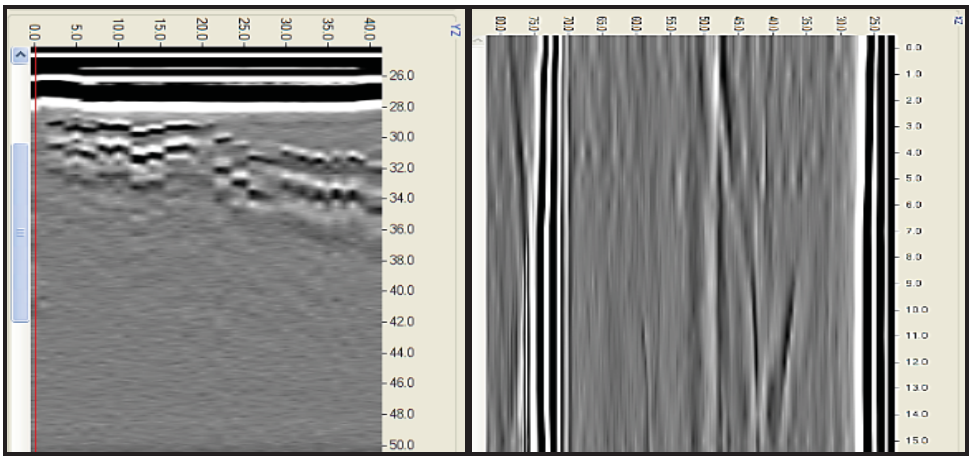

(a) (b)

Fig. 3 Examples of defects found during laser ultrasonic testing (a) a defect at the end face of the specimen, which was in contact with the press plate (b) a defect in the XZ plane, running through the specimen

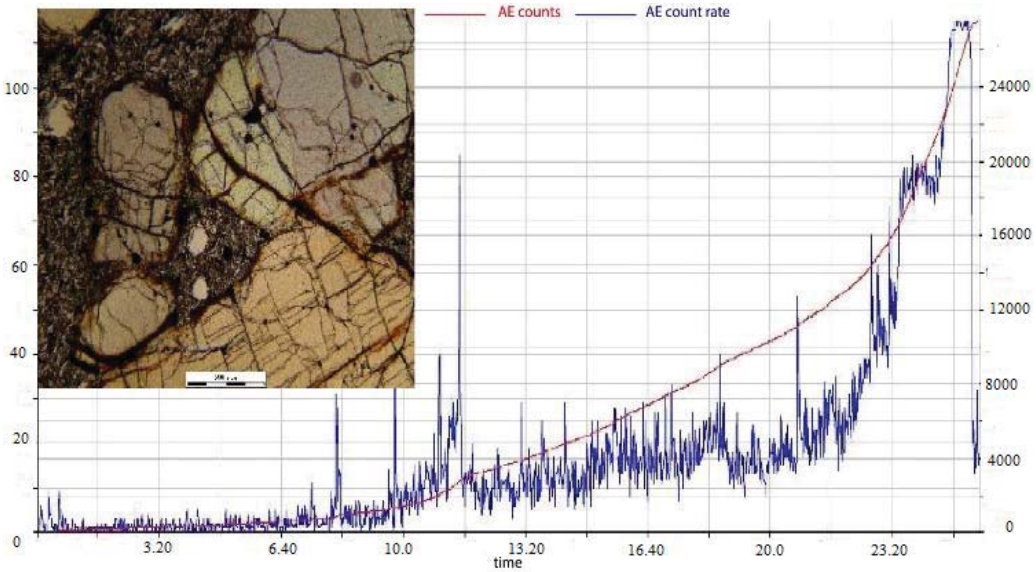

(a)

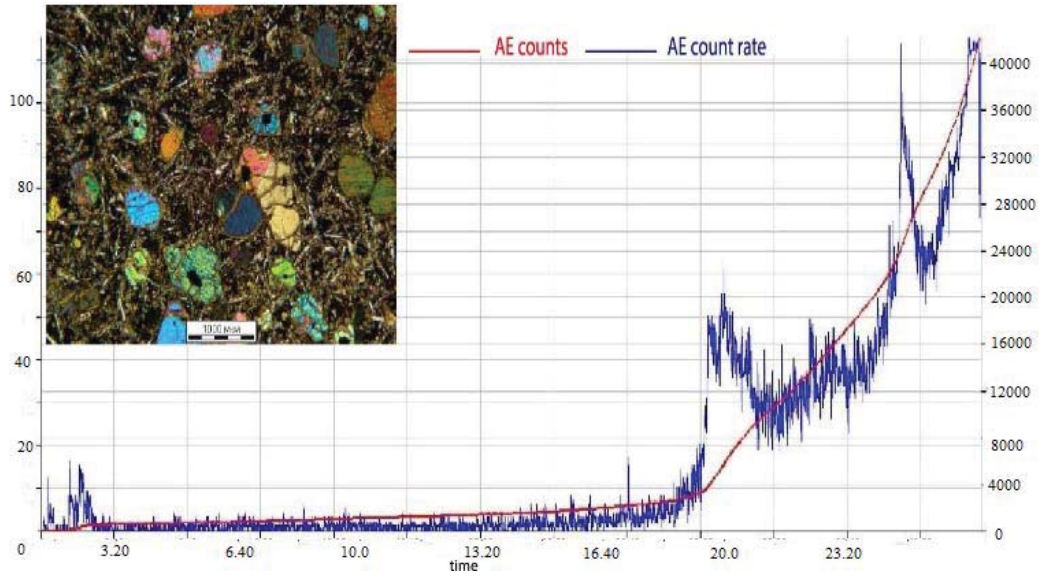

(b)

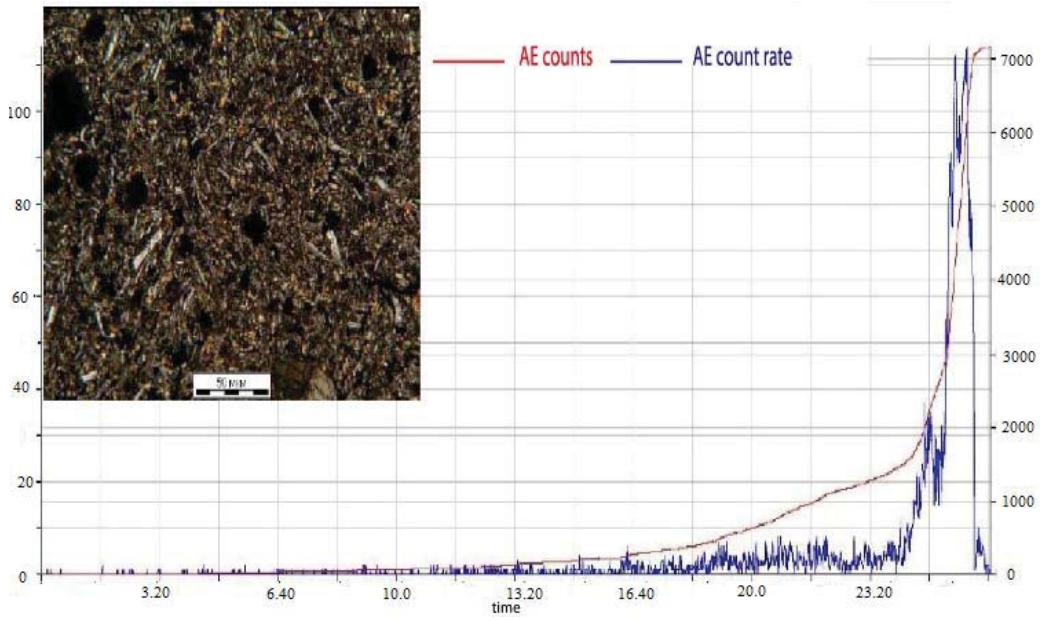

(c)

Fig. 4 Characteristic time dependences of AE counts (red) and AE count rate (blue) for basalts with different structures: (a) coarse, (b) medium-grained, (c) fine-grained

The second type of the curves (Fig. 4 (b)) is characteristic of basalt with microcrystalline texture and smaller amount (15-30%) of unevenly distributed non-fractured olivine phenocrysts 0.3-4 mm in size, which have undergone secondary alterations. Also, plagioclase phenocrysts are observed; they are longer almost tenfold than the plagioclase crystals making up 40% of the groundmass. Ultrafine-grained pyroxene accounts for 60%. This basalt exhibits the smaller value of the maximum energy in the low-frequency band and the greater share of the medium-frequency pulses. The frequency relation remains the same, active emission does not begin immediately, the AE count rate is almost twofold greater than that for the first type. This suggests that the destruction of smaller olivine grains and elongated plagioclase phenocrysts begin when the applied load reaches the breaking strength.

The third type of the curves (Fig. 4 (c)) shows that there is very low activity (4 to 12 AE events per second) in tholeiitic and magnesia basalts practically throughout the test. These rocks host olivine phenocrysts 0.3-1 mm in size (10%), and the groundmass is composed of roughly equal amounts of evenly distributed elongated plagioclase crystals and microlites a few hundredths of millimeter in size. Sometimes plagioclase is weakly oriented. Basalts with this type of

acoustic emissions have a relatively high porosity (up to 19%) as compared to the other studied varieties. The value of stress that causes irreversible deformation resulting in main crack formation and consequent collapse of the basalt specimen can be determined from a sharp change in the angle of the curve. The maximum number of the mid-frequency and high-frequency AE events is by the order of magnitude smaller than that in the rocks characterized by the curves of the first type.

IV Conclusions

The following conclusions can be drawn from the research results:

1) The behavior of a highly homogeneous material under load is non-linear due to the formation of defects; it cannot be described by linear stress-strain equations.
2) Multiple defects and main cracks form at a stress of less than 50% of breaking stress. This means that changes in the properties of the material occur at the early stages of gradual mechanical loading and are related to the changes in the internal structure.

Our findings show that study of the stress-strain behavior of media (even model materials) should take initial anisotropy and the presence of dislocations into account; the initial anisotropy and defects are the cause of changes in the physical and mechanical properties of the media at the early stages of gradual mechanical loading. Such media cannot be described by using the linear theory of elasticity.

Acknowledgment

This work was carried out with financial support from the Ministry of Education and Science of the Russian Federation in the framework of the Increase Competitiveness Program of NUST 'MISiS' (no. K1-2015-025) and the Russian Science Foundation (grant no. 16-17-10181)

References

[1] Brantut, N., Heap, M. J., Meredith, P. G., & Baud, P. (2013). *Time-dependent cracking and brittle creep in crustal rocks: A review*. Journal of Structural Geology, 52, 17-43
[2] Duncan C. Wyllie. *Rock Fall Engineering*. CRC Press, 2014, p. 270
[3] Fusao O., Akira M., Ryosuke U., Sayuri K. Computer Methods and Recent Advances in Geomechanics. CRC Press, 2014, p. 472
[4] The Japanese Society for Non-Destructive Inspection. Practical Acoustic Emission Testing. Springer, 2016, p. 130
[5] Xue, L., Qin, S., Sun, Q., Wang, Y., Min Lee, L., Li, W., 2014. A study on crack damage stress thresholds of different rock types based on uniaxial compression tests. Rock Mech. Rock. Eng. 47, 1183–1195.
[6] Aker, E., Kühn, D., Vavryèuk, V., Soldal, M., Oye, V., Experimental investigation of acoustic emissions and their moment tensors in rock during failure. International Journal of Rock Mechanics & Mining Sciences, 70 (2014) 286-295.
[7] A.A. Karabutov, E.B. Cherepetskaya, Y.G. Sokolovskaya, D.V. Morozov, Study of Effects of Weathering Factors on Internal Structure of Rocks by Laser Ultrasonic Spectroscopy. Applied Mechanics and Materials, vol.843(2016), P.51-58.
[8] A. A. Karabutov, N. B. Podymova, E. B. Cherepetskaya Measuring the Dependence of the local Young's Modulus of isotropic Composite Materials by a pulsed acoustic Method using a Laser Source of Ultrasound, Journal of Applied Mechanics and Technical Physics, Vol. 54, No.3, pp. 500–507, 2013
[9] Ariskin A.A. and Barmina G.S. Modeling Phase Equilibriums at Crystallization of Basalt Magmas, Moscow, Nauka, MAIK Nauka/Interpreriodika, 2000 (in Russian)
[10] Bortnikova S.B., Sharapov V.N., and Bessonova E.P. Geochemical Composition of Thermal Springs in the Donnoye Fumarole Field near the Mutnovsky Volcano, South Kamchatka, and Problems of Relating them to Above-Critical Magmatic Fluids, Dokl. Akad. Nauk, 2007, Vol. 413, No. 4, pp. 530-534
[11] Martynov Yu.A. Perepelov A.B., and Chashchin A.A. Geochemical Typification of the Basaltoids of the Mutnovsky Volcanic Field, South Kamchatka, Tikhookean. Geol., 1995, vol. 14, No.5, pp. 72--83
[12] Martynov Yu.A. and Chashchin A.A. Rock-Forming Minerals of Basic Volcanic Rocks of the Mutnovsky Geothermal Area, in New Data on Petrology of Magmatic and Metamorphic Rocks of Kamchatka, Vladivostok, DVO Akad. Nauk, 1989, pp. 112--128
[13] Selyangin O.B. New Data on the Mutnovsky Volcano: Structure, Evolution, and Prediction, Vulkanol. Seismol., 1993, No.1, pp. 17--35